Original Article

Photoneutron Dose Estimation in GRID Therapy Using an Anthropomorphic Phantom: A Monte Carlo Study

Nahid Chegeni[1], Amir Hossein Karimi[1], Iraj Jabbari[2], Shole Arvandi[3]

[1]Department of Medical Physics, Jundishapur University of Medical Sciences, Ahvaz, Iran, [2]Department of Nuclear Engineering, University of Isfahan, Isfahan, Iran, [3]Department of Radiotherapy and Oncology, Jundishapur University of Medical Sciences, Ahvaz, Iran

N. Chegeni

ORCID ID

https://orcid.org/ 0000-0002-6373-5456

A H. Karimi

ORCID ID

https://orcid.org/0000-0002-1598-8934

Abstract

Background: In the past, GRID therapy was used as a treatment modality for the treatment of bulky and deeply seated tumors with orthovoltage beams. Now and with the introduction of megavoltage beams to radiotherapy, some of the radiotherapy institutes use GRID therapy with megavoltage photons for the palliative treatment of bulky tumors. Since GRID can be a barrier for weakening the photoneutrons produced in the head of medical linear accelerators (LINAC), as well as a secondary source for producing photoneutrons, therefore, in terms of radiation protection, it is important to evaluate the GRID effect on photoneutron dose to the patients. **Methods:** In this study, using the Monte Carlo code MCNPX, a full model of a LINAC was simulated and verified. The neutron source strength of the LINAC (Q), the distributions of flux (ϕ), and ambient dose equivalent (H*[10]) of neutrons were calculated on the treatment table in both cases of with/without the GRID. Finally, absorbed dose and dose equivalent of neutrons in some of the tissues/organs of MIRD phantom were computed with/without the GRID. **Results:** Our results indicate that the GRID increases the production of the photoneutrons in the LINAC head only by 0.3%. The calculations in the MIRD phantom show that neutron dose in the organs/tissues covered by the GRID is on average by 48% lower than conventional radiotherapy. In addition, in the uncovered organs (by the GRID), this amount is reduced to 25%. **Conclusion:** Based on the findings of this study, in GRID therapy technique compared to conventional radiotherapy, the neutron dose in the tissues/organs of the body is dramatically reduced. Therefore, there will be no concern about the GRID effect on the increase of unwanted neutron dose, and consequently the risk of secondary cancer.

Keywords: *GRID therapy, linear accelerator, MIRD phantom, Monte Carlo simulation, photoneutron contamination*

Introduction

GRID therapy or spatially fractionated radiotherapy is a treatment modality, in which a high dose of radiation (15–20 Gy) in a single fraction is given to the tumor. This technique previously was used to treat bulky and deeply seated tumors with orthovoltage beams.[1,2] These tumors should be irradiated under large field sizes that cause significant damage to the skin and normal tissue surrounding the tumor.[3,4] Using GRID therapy allowed to reduce the amount of damage by shielding a part of the field and turning it into a large number of small fields.[2-5] By introducing linear accelerators (LINACs) in the field of radiotherapy that enables to produce megavoltage beams with advantages such as good skin sparing, less scattering, sharp field edges, small penumbra and uniform spatial dose distribution,[6] the use of orthovoltage beams and subsequently GRID therapy were stopped. However, studies have recently been conducted to suggest that GRID therapy with megavoltage photons can be useful in palliative treatments of bulky tumors or in treating tumors that do not respond well to conventional radiotherapy.[7-10]

Despite the advantages mentioned for megavoltage therapies, there has always been concern about the unwanted production of photoneutrons by LINAC head in treating with energies above 10 MeV. The dominant mechanism in the production of photoneutrons by the LINAC head component is the giant dipole resonance process (γ, n). In other words, when the energy of the photon is greater than the energy necessary to separate the last of the nucleus neutron, the photon is able to divide its energy between nucleons and separate a neutron from it, which

How to cite this article: Chegeni N, Karimi AH, Jabbari I, Arvandi S. Photoneutron dose estimation in GRID therapy using an anthropomorphic phantom: A Monte Carlo study. J Med Sign Sens 2018;8:175-83.

Address for correspondence:
Mr. Amir Hossein Karimi, Department of Medical Physics, Jundishapur University of Medical Sciences, Ahvaz, Iran.
E-mail: amir.h.karimi1991@gmail.com, karimi.ah@ajums.ac.ir

Website: www.jmss.mui.ac.ir
DOI: 10.4103/jmss.JMSS_13_18

is less bounded to the nucleus than other neutrons. Such neutrons are called evaporation neutrons. In addition, the incoming photon can directly give its energy to a neutron and cause its separation from the nucleus. Such neutrons will be called knock-on neutrons.[11,12]

Some parts of the LINAC head such as target, primary collimator, secondary collimator, and jaws are made up of elements with high atomic numbers, such as tungsten and lead. The average threshold energy of these elements for the occurrence of the (γ, *n*) interactions is low, respectively, 7.45 and 7.40 MeV,[13] which results in the production of a significant amount of photoneutrons in the LINAC head. Since the energies of these photoneutrons lie in the fast neutron region and also the fast neutrons have higher radiation-weighting factors, they can raise the secondary cancer risk in the patients, endangering their health in the long run.[14,15] This problem is more worrying in modern radiotherapy techniques, in which more monitor units (MU) are used to treat,[16-19] such as intensity-modulated radiotherapy and GRID therapy. In GRID therapy, GRID can be both a source for photoneutrons production and an obstacle to weakening them.

So far, several studies have been carried out on the effect of various components of the LINAC head, including multileaf collimators, flattening filter, wedge and compensator, on photoneutron contamination.[19-22] However, the effect of the GRID on photoneutron contamination has not been completely studied. Although, by measuring, Wang *et al*.[23] showed that in GRID therapy with 18-MV photon beams, neutron dose equivalent received by the patient is on average 35.3% lower conventional radiotherapy (when the same MU and treatment field size are used). So far the effects of GRID on the neutron source strength of LINAC and the distribution of neutron dose on the treatment table have not been studied. In addition, one of the limitations of neutron dosimeters is that even with the most precise tools, one cannot achieve uncertainty <10% in measurements.[24] While by Monte Carlo (MC) simulations, these limitations can be removed very much and a more accurate estimate of neutron dose can be provided. Therefore, in this study, using the MC method, the absorbed dose and dose equivalent of neutrons in some of the organs/tissues of the MIRD phantom were evaluated during irradiation of an abdominal bulky tumor with/without the GRID. Finally, neutron dose in GRID therapy was compared to conventional radiotherapy in order to consider its radiation protection aspects.

Materials and Methods

Geometry and libraries for Monte Carlo simulation

In this study, the MC code MCNPX, Version 2.6,[25] was used to evaluate the effect of GRID on the photoneutrons produced during GRID therapy with 18-MV photon beams. For this purpose, the main components of the Varian Clinac 2100 C/D (California, Varian Medical Systems, USA), including the target, primary collimator, flattening filter, ion chamber, mirror, secondary collimator, jaws, and upper circle, were simulated. Figure 1 shows a two-dimensional view of simulated geometry. In this figure, besides the main parts of the LINAC head, the MIRD phantom and the GRID under study are also simulated.

The simulated GRID is made by the .decimal company. (.decimal Inc., Sanford, FL, USA) and its profile was extracted from the Wang *et al*.'s study.[23] The genus of the GRID is brass (63% copper and 37% zinc) and has a thickness of 7.62 cm. The conical holes of this GRID follow direction of radiation divergence. Each hole creates a circular field at the isocenter (IC) with a diameter of 1 cm. The centers of holes are 2 cm apart. The distance from the floor of the GRID to the IC is 30.78 cm.

In the simulations, cross-section libraries of ENDF/B-V2.0, MCPLIB04, and EL03 were used to consider neutron, photon, and electron interactions with matter, respectively. These interactions include absorption, dispersion and capture for neutrons, Rayleigh and Compton scattering, pair production and the photoelectric effect for photons and ultimately elastic, inelastic collision, and Bremsstrahlung for electrons. It is worth mentioning that the LA150u, KAERI01u, and CNDC01u cross-section libraries were used to consider the production of photoneutrons.

Percentage depth doses and profiles benchmarking

Before the transmission of photoneutrons, the calculated dose distributions should be validated by those obtained from the measurements. For this purpose, the percentage depth dose (PDD) and profile curves were measured by an ionization chamber (CC13, Scanditronix Wellhofer, Germany) with a sensitive volume of 0.13 cm^3 in the Scanditronix blue phantom. The uncertainty in the position accuracy of the phantom scan system was ±0.1 mm.

For MC calculations, the electron beams, which both their energy distribution and spatial distribution were Gaussian,

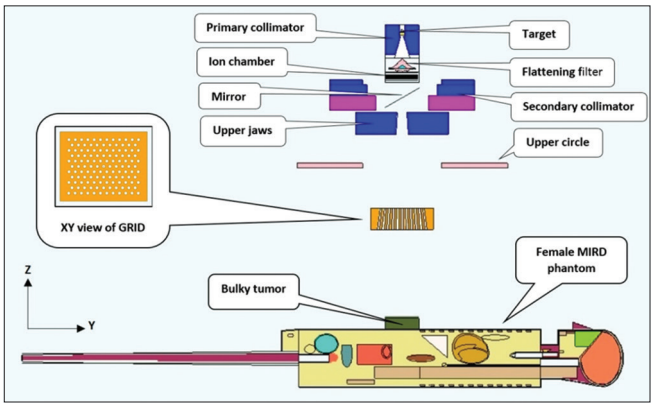

Figure 1: The YZ view of the simulated geometry consisting of the main parts of the linear accelerator head, GRID, and MIRD phantom (in this figure, a cylinder of water with 4 cm- height and 5 cm- radius was placed at the source to surface distance of 100 cm as a typical abdominal tumor)

were simulated as the electron source impinging to the target. While the full width at half maximum (FWHM) of energy distribution for the electron beams were fixed at 1.2 MeV, the average energy and FWHM of spatial distribution were adjusted so that for each of the 4 cm × 4 cm, 10 cm × 10 cm, and 20 cm × 20 cm field sizes, the calculated and measured curves can be consistent with together. For this purpose, the criteria of 2 mm and 2% for Gamma index function were applied, then calculated and experimental dose distributions were compared together. Gamma index >1 means no agreement and Gamma index <1 means the existence of an acceptable agreement between the results of the simulation and measurement under the 2 mm and 2% criteria.[26] Gamma index values were calculated based on its mathematical definition using MATLAB software. The use of MATLAB code for calculating Gamma index has already been reported in the Sadoughi *et al*.'s study.[27]

To calculate PDD and profile curves, a 50 cm × 50 cm × 50 cm water phantom was simulated at the source to surface distance (SSD) of 100 cm. Using *F8 tally, PDDs were calculated in the central axis voxels to a depth of 30 cm. Dose profiles were also calculated at the 10 cm depth in the cross-line direction. In these calculations, the electron and photon energy Cut-offs were considered to be 0.7 and 0.01 MeV, respectively. In calculating the PDD and profile curves, 2 × 10^9 electron histories were recorded to obtain relative statistical uncertainties <1%. All computer calculations in this study were carried out by a 64-core CPU paralleled at the University of Isfahan, Isfahan, Iran.

As a point at the end of this section, since the MCNP code normalizes the results of the calculations for photoneutrons to an electron exiting from the source, therefore, it is better for comparison purposes that these quantities are reported in terms of 1 Gy of photon dose in the water phantom d_{max}. For this reason, the number of electrons needed to deliver 1 Gy of photon dose to d_{max} was calculated in the standard conditions (SSD = 100 cm, field size = 10 cm × 10 cm). This factor is then multiplied by the calculated quantities for photoneutrons to be reported according to 1 Gy of photon dose delivered to d_{max}.

The effect of the GRID on photoneutron contamination

After the correct tuning of the electron beams, the neutron mode was added to the programs. Furthermore, the fourth input parameter in the PHYS: P card was set in a bias state to reduce the relative statistical uncertainty in calculations in addition to allowing photoneutrons production interactions. Besides, in order to expedite the calculation process, the electron and photon energy Cut-offs were placed to be 6 MeV. This amount is lower than the average threshold energy of photoneutrons production for lead (7.40 MeV). In these calculations, the number of 2 × 10^9 electron histories was traced so that the relative statistical uncertainties would be less than 1%. All calculations performed in this section are limited to the 10 cm × 10 cm treatment field size.

To evaluate the GRID effect on the photoneutrons production, the neutron source strength of the LINAC in both cases, without/with the GRID, was calculated by the method provided by McGinley and Landry.[28] Accordingly, using F1 tally, the neutron flux on a sphere with the center of the LINAC target and with a radius of 100 cm was calculated for 1 Gy of photon dose delivered to d_{max}.

Using F5 tally and En card, the neutron energy spectra at the IC was calculated in two modes: with/without the walls of the treatment room. Figure 2 shows the geometry of the simulated treatment room, which is related to the Golestan Hospital, Ahvaz, Iran. The walls of this room are made up of ordinary concrete with a density of 2.35 g/cm^3. The weight percentages of constituent elements of this concrete have been extracted from the National Council on Radiation Protection and Measurements, Report No. 49.[29] Afterward, with considering the walls of the treatment room, the photoneutrons spectra was calculated at the IC in two modes: With/without the GRID. In these calculations, the energy bin (10^{-9}, 10 MeV) was divided into 100 intervals logarithmically. It should be noted that in calculating the spectra, the mean relative statistical uncertainty of neutron flux was <1.3% on all of 100 energy intervals.

Using F5 tally, DF card and the flux-to-dose rate conversion factors of the International Commission on Radiological Protection (ICRP), Report No. 74,[30] the flux and equivalent dose of neutrons were calculated at the IC and at a number of points located on the treatment table in two modes: With/without the GRID.

The MC simulation has the power to provide an acceptable dose estimate in cases where it is not possible to measure, or measurements have high uncertainty. For example, in the study of photoneutron dose which the patients receive during radiotherapy. Therefore, to more accurately assess the GRID effect on neutron dose in the sensitive tissues/organs, the revised female MIRD phantom was included in the simulation. In addition, a 4 cm thick, water-filled

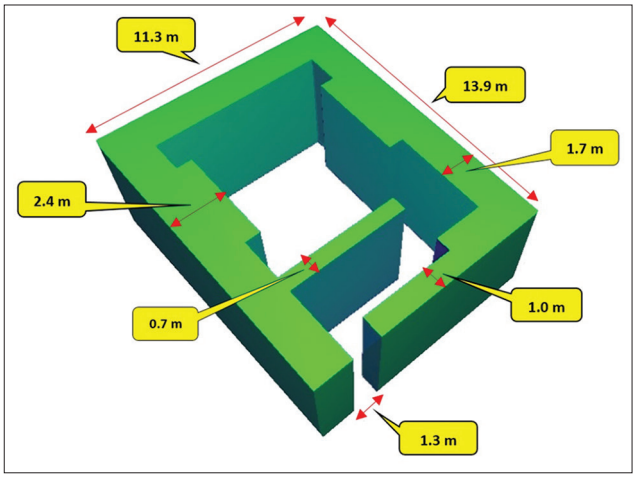

Figure 2: Treatment Room Geometry of Golestan Hospital, Ahvaz, Iran

cylinder with a 5 cm radius (as a typical bulky tumor) was added on the phantom abdomen. This tumor was placed at SSD = 100 cm [Figure 1].

Using F4 tally and the flux-to-dose rate conversion factors of ICRP, Report No. 74,[30] the neutron dose equivalent, in two conditions: With/without the GRID, was calculated in a number of MIRD phantom organs/tissues. In addition, using F6 tally, the absorbed dose of neutrons in the same organs/tissues was calculated (with/without GRID). In these calculations, 2×10^{10} electron histories were used to achieve an acceptable relative statistical uncertainty. It is worth noting that to take into account the interaction of the thermal neutrons with water in the MIRD phantom, cross-section library of lwtr.01t was used.

Results

To benchmark the simulated model, different average energies and spatial FWHM were used for the electron beams. In each case, calculated PDD and profile curves were compared with related experimental curves (by Gamma index function) to choose from among them the optimum average energy and spatial distribution of electron beams. This optimum mode was found in an average energy of 18.3 MeV and a 1.4 mm spatial FWHM.

Figure 3a shows the calculated and measured PDDs for each of the 4 cm × 4 cm, 10 cm × 10 cm, and 20 cm × 20 cm field sizes. From this figure, we can also see that calculated and measured curves fit well into each other.

In Figure 3b, the calculated Gamma index values were given for PDDs. In this figure, the Gamma index values at all points (except the buildup region) are <1 which means that calculated and measured PDDs are agreed under the 2 mm and 2% criteria. In the buildup region, for a small number of points, the Gamma index values have not been passed (>1), which is expected due to a sharp increase in the collected charges and thus insensitivity of the ionization chamber. In some studies, similar reasons were mentioned for the existence of small differences between calculated and measured curves.[31,32]

Figure 4a shows the profile curves calculated and measured for 4 cm × 4 cm, 10 cm × 10 cm, and 20 cm × 20 cm field sizes at the 10 cm depth in the water phantom (in the cross-line direction). The calculated Gamma index values for them are given in Figure 4b which shows Gamma index values have been passed for 4 cm × 4 cm and 10 cm × 10 cm field sizes at all points. In the 20 × 20 field size, the Gamma index value is not passed only for a single point, which can be ignored.

The sum of the above findings confirms that our model is valid under the optimum conditions selected for electron beams. For this model, the number of electrons needed to deliver 1 Gy of photon dose to d_{max} was estimated to be 1.26×10^{15} electrons per Gy, which is comparable with the value obtained by Martínez-Ovalle *et al*.[33] (1.52×10^{15} electron per Gy).

Table 1 summarizes the flux and ambient dose equivalent of neutrons for a number of points located on the treatment table. It is noticeable, these values related to the non-GRID mode.

The neutron source strength of the LINAC in both modes of without/with the GRID was 1.378×10^{12} *n*/Gy and 1.382×10^{12} *n*/Gy, respectively. In fact, the GRID increases the neutron source strength by only 0.3%.

Figure 5 presents the photoneutrons spectra at the IC, by including the treatment room in the simulation and without it. Both of these spectra are obtained in the open-field state (i.e., without the GRID). As shown in this figure,

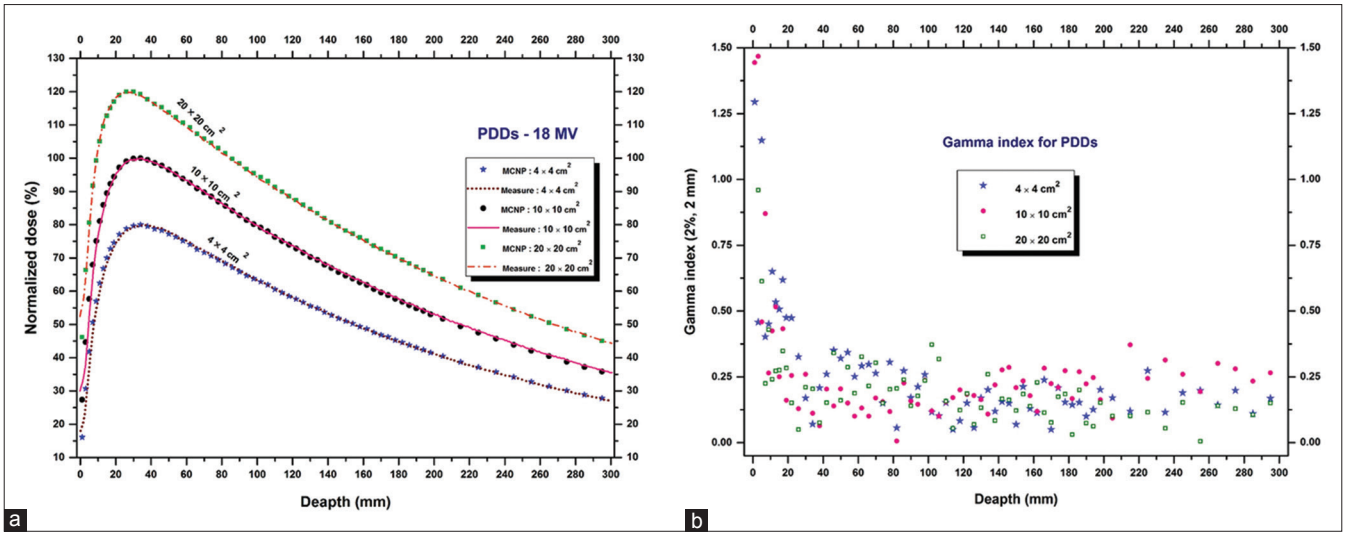

Figure 3: (a) The PDD curves calculated and measured in 4 cm × 4 cm, 10 cm × 10 cm, and 20 cm × 20 cm field sizes (to avoid overlapping them, PDD values for 4 cm × 4 cm, 10 cm × 10 cm, and 20 cm × 20 cm field sizes have been multiplied by 0.8, 1, and 1.2, respectively). (b) Gamma index values for evaluating the agreement between calculated and measured PDDs in 4 cm × 4 cm, 10 cm × 10 cm, and 20 cm × 20 cm field sizes. PDD: Percentage depth dose

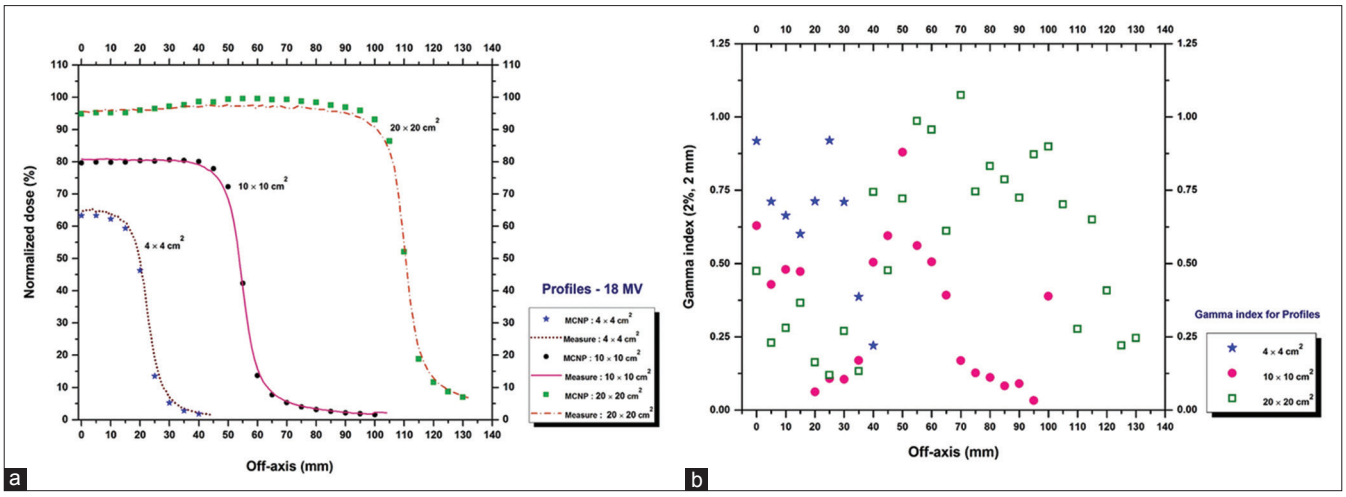

Figure 4: (a) The profile curves calculated and measured in 4 cm × 4 cm, 10 cm × 10 cm, and 20 cm × 20 cm field sizes at the 10 cm depth in the water phantom (in the cross-line direction). (b) Gamma index values for evaluating the agreement between calculated and measured profiles in 4 cm × 4 cm, 10 cm × 10 cm, and 20 cm × 20 cm field sizes

Table 1: Comparison between the results of this study and literature in calculating the flux and the ambient dose equivalent of neutrons on the treatment table

Distance from IC (cm)	ϕ (10^7 n/cm²/Gy)		Relative differences (%)	(H*(10)) (mSv/Gy)		Relative differences (%)
	This study	Literature		This study	Literature	
0	1.684±0.002	1.58 Howell *et al*.[19]	6.6	3.936±0.004	3.70 Mohammadi *et al*.[34]	6.4
10	1.218±0.002	-	-	2.329±0.003	2.05 d'Errico *et al*.[35]	13.6
20	1.100±0.001	-	-	1.994±0.003	1.75 d'Errico *et al*.[35]	13.9
50	0.900±0.001	0.979 Králík *et al*.[36]	−8.1	1.483±0.002	1.212 Králík *et al*.[36]	22.4
100	0.694±0.001	0.59 Alem-Bezoubiri *et al*.[37]	17.6	0.938±0.001	0.65[a] Alem-Bezoubiri *et al*.[37]	44.3

[a]Alem-Bezoubiri *et al*. reported 0.62 directly in their results table, but in the same study, they showed that without considering the MLCs, this value would be increased to 0.65. IC – Isocenter; MLCs – Multileaf collimators

with considering the walls of the treatment room in the simulations, two long and short peaks are seen in the spectrum, respectively, in the region of fast and thermal neutrons. In contrast, with the removal of walls from the simulations, while the peak of the fast neutrons remains nearly unchanged, the peak of the thermal neutron disappears from the spectrum.

The effect of the GRID on the shape of the photoneutrons spectrum (at the IC) is shown in Figure 6. From this figure, we can observe that the GRID reduces only the flux of the fast neutrons and does not change in the other areas of the spectrum. Using these spectra, the mean energy of neutrons at the IC was calculated in two modes: Without/with the GRID, which was 0.72 and 0.66 MeV, respectively.

In Figure 7a and b, respectively, the flux and the ambient dose equivalent of neutrons on the treatment table are compared for two conditions: with/without the GRID. From these figures, it can see that the GRID reduces the flux and the ambient dose equivalent of neutrons at the IC, respectively, 41.0% and 48.9%. Furthermore, the average reduction in the flux and the ambient dose equivalent of neutrons at the intervals of <30 cm from the IC are, respectively, 29.5% and 38.5%, while at the intervals 30 cm far away from the IC, the GRID increases the flux and the ambient dose equivalent of neutrons, respectively, 1.7% and 3.8%.

Table 2 estimates the absorbed dose and dose equivalent of neutrons calculated in a number of organs/tissues of the MIRD phantom. In each case and for each organ/tissue, the relative differences between the GRID mode and the non-GRID mode have been reported. In these calculations, the mean relative statistical uncertainties for the absorbed and equivalent dose of neutrons, were 3.1% and 2.4%, respectively. It should be noted that for a very small number of the organs/tissues, the relative statistical uncertainties were large, which their maximum belonged to the adrenals (11.4% and 8.8%, respectively).

Discussion

The neutron source strength of the LINAC in the non-GRID mode was 1.378×10^{12} *n*/Gy, which is acceptably different from the value of 1.3×10^{12} *n*/Gy calculated by Mesbahi *et al*.;[38] in addition, the value of 1.2×10^{12} *n*/Gy calculated by Mao *et al*.[39] (respectively, 6.0% and 14.8%). Since in these studies, the energy of electron beams, the type of MC tools, cross-section libraries for photoneutrons production, and the amount of available details from the LINAC head were different.

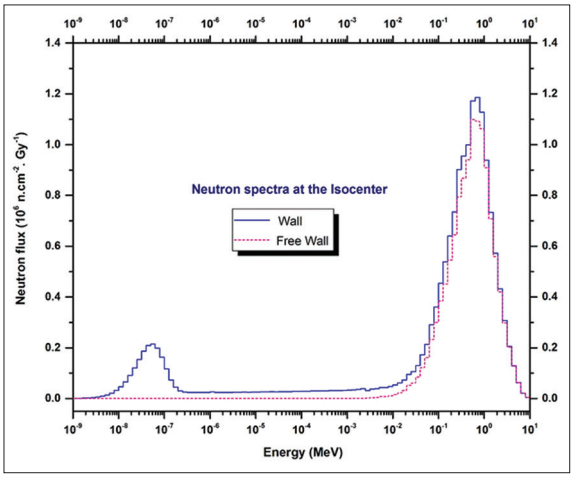

Figure 5: The photoneutrons spectra at the isocenter (in the air) with considering the walls of the treatment room and without them

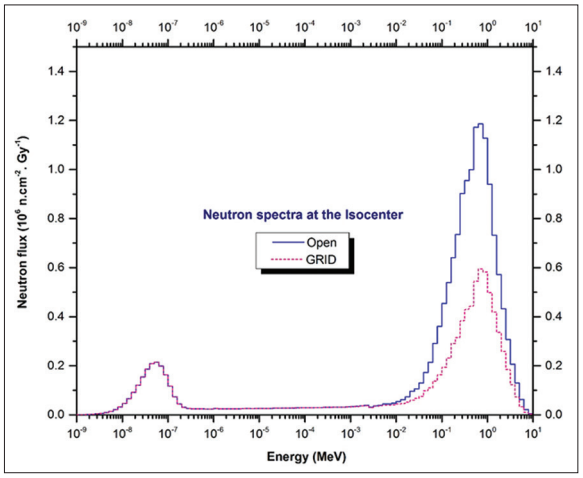

Figure 6: The photoneutrons spectra at the isocenter (in the air) with/without the GRID

Table 2: The absorbed dose and equivalent dose of neutrons calculated in different organs/tissues of the MIRD phantom in two modes: With and without the GRID

Tissue/organ	Neutron absorbed dose (mGy/Gy)		Relative differences (%)	Neutron equivalent dose (mSv/Gy)		Relative differences (%)
	Open	GRID		Open	GRID	
Adrenals	0.0058±0.0006	0.0035±0.0004	−39.7	0.121±0.010	0.080±0.007	−33.9
Brain	0.0129±0.0002	0.0133±0.0002	3.1	0.254±0.003	0.261±0.003	2.8
Breast	0.0795±0.0007	0.0680±0.0007	−14.5	1.281±0.010	1.090±0.010	−14.9
Colon	0.0234±0.0003	0.0134±0.0003	−42.7	0.478±0.005	0.275±0.004	−42.5
Cranium	0.0146±0.0002	0.0150±0.0002	2.7	0.364±0.004	0.373±0.004	2.5
Eyes	0.0531±0.0019	0.0563±0.0020	6.0	0.983±0.033	1.038±0.034	5.6
Gall bladder	0.0290±0.0010	0.0132±0.0007	−54.5	0.560±0.015	0.261±0.010	−53.4
Heart	0.0288±0.0004	0.0212±0.0004	−26.4	0.571±0.007	0.417±0.006	−27.0
Intestine	0.0207±0.0003	0.0112±0.0002	−45.9	0.419±0.004	0.230±0.003	−45.1
Kidneys	0.0064±0.0002	0.0040±0.0002	−37.5	0.128±0.003	0.088±0.003	−31.3
Liver	0.0293±0.0003	0.0166±0.0002	−43.3	0.576±0.005	0.331±0.003	−42.5
Lungs	0.0189±0.0002	0.0154±0.0002	−18.5	0.376±0.003	0.306±0.003	−18.6
Mandible and teeth	0.0294±0.0005	0.0308±0.0005	4.8	0.725±0.010	0.756±0.011	4.3
Ovaries	0.0114±0.0010	0.0078±0.0008	−31.6	0.248±0.015	0.164±0.012	−33.9
Pancreas	0.0152±0.0005	0.0079±0.0004	−48.0	0.309±0.008	0.166±0.006	−46.3
Pelvis	0.0062±0.0001	0.0049±0.0001	−21.0	0.174±0.002	0.139±0.002	−20.1
Rectum	0.0099±0.0006	0.0082±0.0005	−17.2	0.214±0.009	0.184±0.008	−14.0
Ribs	0.0288±0.0001	0.0228±0.0001	−20.8	0.705±0.003	0.561±0.003	−20.4
Skin	0.0468±0.0001	0.0418±0.0001	−10.7	0.836±0.001	0.747±0.001	−10.6
Spine	0.0046±0.0001	0.0035±0.0001	−23.9	0.125±0.002	0.101±0.002	−19.2
Spleen	0.0082±0.0004	0.0057±0.0003	−30.5	0.173±0.006	0.123±0.005	−28.9
Stomach	0.0416±0.0006	0.0223±0.0004	−46.4	0.805±0.009	0.436±0.007	−45.8
Thymus	0.0563±0.0016	0.0531±0.0016	−5.7	1.041±0.026	0.965±0.025	−7.3
Thyroid	0.0206±0.0010	0.0209±0.0010	1.5	0.408±0.016	0.414±0.016	1.5
Tumor	0.1867±0.0014	0.0789±0.0009	−57.7	2.985±0.021	1.274±0.014	−57.3
Urinary bladder	0.0358±0.0007	0.0279±0.0006	−22.1	0.700±0.011	0.545±0.010	−22.1
Uterus	0.0172±0.0008	0.0112±0.0007	−34.9	0.358±0.013	0.235±0.010	−34.4

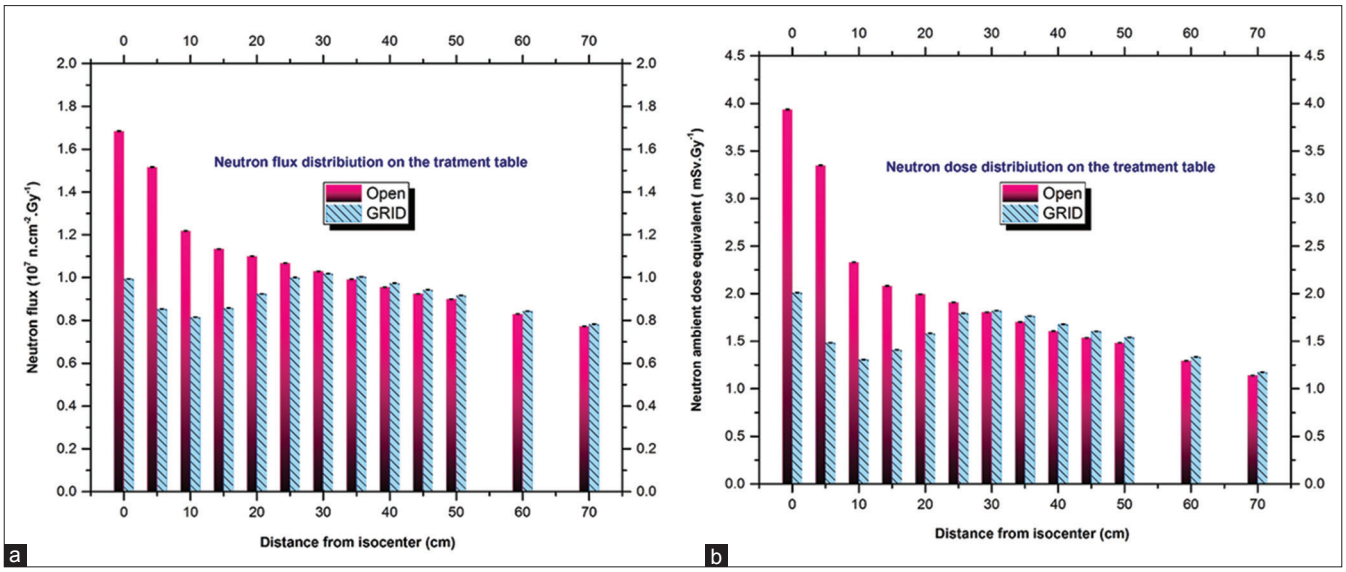

Figure 7: (a) The distribution of the neutron flux on the treatment table (in terms of distance from the isocenter). (b) The distribution of the neutron ambient dose equivalent on the treatment table (in terms of distance from the isocenter)

In the presence of the GRID, the neutron source strength of the LINAC reached to 1.382×10^{12} *n*/Gy and increased only 0.3%, which is negligible in comparison to the contribution of other components of the LINAC head in photoneutrons production.[39] Therefore, the GRID does not significantly increase the production of photoneutrons, and consequently, there is no concern about the increase of neutron dose in patients treated with the GRID therapy technique. However, the GRID effect on the scattering of neutrons toward the treatment table should be evaluated.

From Table 1, one can note a good agreement achieved between the obtained results and the related values in the literature.[19,34-37] It can also see, the average relative difference of our results with literature is 5.4% and 20.1% for the flux and the ambient dose equivalent of neutrons, respectively. These differences are reasonable, because the type of study (measurement/simulation), cross-section libraries for photoneutrons production, as well as the treatment room geometries differed. These comparisons indicate that our model is reliable for transmission of the photoneutrons on the treatment table.

As Figure 5 shows, if the walls of the treatment room are removed from the simulations, thermal neutrons do not appear in the spectrum which is in agreement with the study conducted by Mohammadi *et al*.[14] (i.e., the origin of thermal neutrons in the spectrum is the walls of the treatment room, not the LINAC head components). For this reason, the presence of GRID does not change the flux and subsequently the dose of neutrons in the thermal region [Figure 6]. This seems in contrast with Wang *et al*.'s results,[23] who showed that the GRID reduced the dose equivalent of thermal neutrons 39.3% (at the IC). The reason for this disagreement could be this point that our calculations were done in the air while their dosimeter was attached to the left buccal side of the RANDO® phantom.

The GRID decreases the average energy of neutrons at the IC from 0.72 to 0.66 MeV and also lowers the neutron flux by 41.0%. For this reason, the ambient dose equivalent of neutrons at the IC is reduced by 48.9%.

In Figure 7a and b, one can see that GRID decreases the flux and ambient dose equivalent of neutrons on average 29.5% and 38.5%, respectively, which are evident only at intervals of <30 cm, from the IC. While the effect of GRID in the variations of flux or dose is negligible at distances >30 cm from the IC. For example, in a 40 cm distance from the IC, the GRID increases the ambient dose equivalent of neutrons approximately 4.5%, from 1.606 ± 0.002 to 1.678 ± 0.003 mSv/Gy. For this reason, as Table 2 shows, the GRID increases the neutron dose only <8% in the organs/tissues located far away from the IC (such as the eyes, thymus, mandible and teeth, brain, cranium, and thyroid), which is ignorable in comparing with the reduction of 48.9% neutron dose at the IC.

From Figure 7b, it can be seen that in the without GRID mode, the ambient dose equivalent of neutrons at the IC is more than the other points on the treatment table. Therefore, the tumor located in the IC receives the most neutron dose. The presence of the GRID causes a high reduction about 60% [Table 2] in neutron dose at the tumor, which reduces the risk of secondary cancer in the treatment volume.

According to Table 2, in the organs/tissues covered by the GRID, including tumor, gallbladder, pancreas, stomach, intestine, liver, and colon, the neutron dose is on average 48% less than conventional radiotherapy, which is comparable with 35.3% reported by Wang *et al*.[23] Also in the organs/tissues which were not covered by the GRID

such as adrenals, kidneys, uterus, ovaries, spleen, heart, spine, urinary bladder, pelvis, ribs, lungs, rectum, and breast, the neutron dose is on average 25% less than the non-GRID mode.

Conclusion

Based on the findings of this study, in GRID therapy technique compared to conventional radiotherapy, the neutron dose in the tissues/organs of the body is dramatically reduced. Therefore, there will be no concern about the GRID effect on the increase of unwanted neutron dose, and consequently, the risk of secondary cancer.

Acknowledgments

The authors would like to thank Dr. Yaser Kasesaz from the Nuclear Science and Technology Research Institute, Dr. Najmeh Mohammadi from the Ferdowsi University of Mashhad, and Mr. Mohammad Nami Nazari for their technical helps.

Financial support and sponsorship

This study is a part of MSc thesis of Amir Hossein Karimi which financially supported by Jundishapur University of Medical Sciences (Grant No. U-97020).

Conflicts of interest

There are no conflicts of interest.

References

1. Jolles B. The study of connective-tissue reaction to radiation; the sieve or chess method. Br J Cancer 1949;3:27-31.
2. Marks H. Clinical experience with irradiation through a grid. Radiology 1952;58:338-42.
3. Jolles B, Mitchell RG. Optimal skin tolerance dose levels. Br J Radiol 1947;20:405-9.
4. Jolles B. X-ray skin reactions and the protective role of normal tissues. Br J Radiol 1941;14:110-2.
5. Harris W. Recent clinical experience with the grid in the x-ray treatment of advanced cancer; preliminary report. Radiology 1952;58:343-50.
6. Das IJ, Kase KR. Higher energy: Is it necessary, is it worth the cost for radiation oncology? Med Phys 1992;19:917-25.
7. Mohiuddin M, Stevens JH, Reiff JE, Huq MS, Suntharalingam N. Spatially fractionated (GRID) radiation for palliative treatment of advanced cancer. Radiat Oncol Invest 1996;4:41-7.
8. Mohiuddin M, Fujita M, Regine WF, Megooni AS, Ibbott GS, Ahmed MM. High-dose spatially-fractionated radiation (GRID): A new paradigm in the management of advanced cancers. Int J Radiat Oncol Biol Phys 1999;45:721-7.
9. Peñagarícano JA, Moros EG, Ratanatharathorn V, Yan Y, Corry P. Evaluation of spatially fractionated radiotherapy (GRID) and definitive chemoradiotherapy with curative intent for locally advanced squamous cell carcinoma of the head and neck: Initial response rates and toxicity. Int J Radiat Oncol Biol Phys 2010;76:1369-75.
10. Neuner G, Mohiuddin MM, Vander Walde N, Goloubeva O, Ha J, Yu CX, *et al*. High-dose spatially fractionated GRID radiation therapy (SFGRT): A comparison of treatment outcomes with cerrobend vs. MLC SFGRT. Int J Radiat Oncol Biol Phys 2012;82:1642-9.
11. Facure A, Falcão RC, Silva AX, Crispim VR, Vitorelli JC. A study of neutron spectra from medical linear accelerators. Appl Radiat Isot 2005;62:69-72.
12. Mohammadi N, Miri-Hakimabad SH, Rafat-Motavalli L. A Monte Carlo study for photoneutron dose estimations around the high-energy linacs. J Biomed Phys Eng 2014;4:127-40.
13. Chadwick M, Oblozinsky P, Blokhin A, Fukahori T, Han Y, Lee Y, *et al*. Handbook on Photonuclear Data for Applications: Cross Sections and Spectra. IAEA TECH-DOC; 2000. p. 1178.
14. Mohammadi N, Miri-Hakimabad H, Rafat-Motavlli L, Akbari F, Abdollahi S. Neutron spectrometry and determination of neutron contamination around the 15 MV Siemens Primus LINAC. J Radioanalytical Nucl Chem 2015;304:1001-8.
15. The recommendations of the international commission on radiological protection. ICRP publication.Ann ICRP 2007;37:1-332.
16. Khosravi M, Shahbazi-Gahrouei D, Jabbari K, Nasri-Nasrabadi M, Baradaran-Ghahfarokhi M, Siavashpour Z, *et al*. Photoneutron contamination from an 18 MV Saturne medical linear accelerator in the treatment room. Radiat Prot Dosimetry 2013;156:356-63.
17. Shahbazi-Gahrouei D, Khosravi M, Jabbari K, Gheisari R. Measurement of photoneutron dose in the linear accelerator at the radiation therapy section of Seyed-Al-Shohada Hospital, Isfahan, Iran. J Isfahan Med Sch 2012;29:2330-9.
18. Becker J, Brunckhorst E, Schmidt R. Investigation of the neutron contamination in IMRT deliveries with a paired magnesium and boron coated magnesium ionization chamber system. Radiother Oncol 2008;86:182-6.
19. Howell RM, Ferenci MS, Hertel NE, Fullerton GD. Investigation of secondary neutron dose for 18 MV dynamic MLC IMRT delivery. Med Phys 2005;32:786-93.
20. Hashemi SM, Hashemi-Malayeri B, Raisali G, Shokrani P, Sharafi AA, Torkzadeh F. Measurement of photoneutron dose produced by wedge filters of a high energy linac using polycarbonate films. J Radiat Res 2008;49:279-83.
21. Mesbahi A. A Monte Carlo study on neutron and electron contamination of an unflattened 18-MV photon beam. Appl Radiat Isot 2009;67:55-60.
22. Rezaian A, Nedaie HA, Banaee N. Measurement of neutron dose in the compensator IMRT treatment. Appl Radiat Isot 2017;128:136-41.
23. Wang X, Charlton MA, Esquivel C, Eng TY, Li Y, Papanikolaou N. Measurement of neutron dose equivalent outside and inside of the treatment vault of GRID therapy. Med Phys 2013;40:093901.
24. Chibani O, Ma CM. Photonuclear dose calculations for high-energy photon beams from Siemens and Varian linacs. Med Phys 2003;30:1990-2000.
25. Pelowitz D. MCNPXTM user's manual, version 2.6. 0. Los Alamos National Laboratory report LA-CP-07-1473. 2008.
26. Low DA, Harms WB, Mutic S, Purdy JA. A technique for the quantitative evaluation of dose distributions. Med Phys 1998;25:656-61.
27. Sadoughi HR, Nasseri S, Momennezhad M, Sadeghi HR, Bahreyni-Toosi MH. A comparison between GATE and MCNPX Monte Carlo codes in simulation of medical linear accelerator. J Med Signals Sens 2014;4:10-7.
28. McGinley PH, Landry JC. Neutron contamination of x-ray beams produced by the Varian Clinac 1800. Phys Med Biol 1989;34:777.

29. NCRP. Structural Shielding Design and Evaluation for Medical use of x Rays and Gamma Rays of Energies up to 10 MeV. NCRP Report 49. Bethesda MD: NCRP; 1976.
30. Conversion coefficients for use in radiological protection against external radiation. Adopted by the ICRP and ICRU in September. Ann ICRP 1996;26:1-205.
31. Jabbari K, Anvar HS, Tavakoli MB, Amouheidari A. Monte Carlo simulation of siemens ONCOR linear accelerator with BEAMnrc and DOSXYZnrc code. J Med Signals Sens 2013;3:172-9.
32. Atarod M, Shokrani P. Monte Carlo study of fetal dosimetry parameters for 6 MV photon beam. J Med Signals Sens 2013;3:31-6.
33. Martínez-Ovalle SA, Barquero R, Gómez-Ros JM, Lallena AM. Neutron dose equivalent and neutron spectra in tissue for clinical linacs operating at 15, 18 and 20 MV. Radiat Prot Dosimetry 2011;147:498-511.
34. Mohammadi A, Afarideh H, Abbasi Davani F, Ghergherehchi M, Arbabi A. Monte Carlo study of neutron-ambient dose equivalent to patient in treatment room. Appl Radiat Isot 2016;118:140-8.
35. d'Errico F, Nath R, Tana L, Curzio G, Alberts WG. In-phantom dosimetry and spectrometry of photoneutrons from an 18 MV linear accelerator. Med Phys 1998;25:1717-24.
36. Králík M, Turek K, Vondrácek V. Spectra of photoneutrons produced by high-energy X-ray radiotherapy linacs. Radiat Prot Dosimetry 2008;132:13-7.
37. Alem-Bezoubiri A, Bezoubiri F, Badreddine A, Mazrou H, Lounis-Mokrani Z. Monte Carlo estimation of photoneutrons spectra and dose equivalent around an 18 MV medical linear accelerator. Radiat Phys Chem 2014;97:381-92.
38. Mesbahi A, Ghiasi H, Mahdavi SR. Photoneutron and capture gamma dose equivalent for different room and maze layouts in radiation therapy. Radiat Prot Dosimetry 2010;140:242-9.
39. Mao XS, Kase KR, Liu JC, Nelson WR, Kleck JH, Johnsen S. Neutron sources in the Varian Clinac 2100C/2300C medical accelerator calculated by the EGS4 code. Health Phys 1997;72:524-9.

BIOGRAPHIES

Nahid Chegeni received the master's degree in Medical Physics in 2002 from Iran Medical Science University, Tehran and PhD degree in Medical Physics in 2013 from Ahvaz Jundishapur University of Medical Sciences. Her research interests are radiotherapy, dosimetry, Monte Carlo simulation, and imaging in radiotherapy.

Email: chegenin@gmail.com

Amir Hossein Karimi is the MSc student of Medical Physics at the Jundishapur University of Medical Sciences, Ahvaz, Iran. He received his BSc degree in Physics in 2016 from Isfahan University of Technology (IUT), Isfahan, Iran.
Now, his research interests are in the field of Radiotherapy, Radiation Protection, Neutron dosimetry and Monte Carol calculations.

Email: amir.h.karimi1991@gmail.com

Iraj Jabbari received his MSc degree in Medical Radiation Engineering in 1999 from Sharif University of Technology, Tehran, Iran and his PhD degree in 2011 in Medical Radiation Engineering from Shahid Beheshti University, Tehran, Iran.
Now, he is assistant professor of nuclear engineering at the University of Isfahan, Isfahan, Iran.

Email: i_jabbari@ast.ui.ac.ir

Shole Arvandi received General Medicine and M.D. in Radiation Oncology in 1996 from Tehran Medical Science University. Her research interests are investigating factors and the role of stage associated with malignancy and the pathology of malignancies in the prognosis.

Email: arvandish@yahoo.com